

Modelling and analysis of linear DC motor with constant thrust characteristics

Raja Nor Firdaus Kashfi Raja Othman^{1,2}, Siti Zulaika Mat Isa^{1,2}, Nor Aishah Md. Zuki^{1,2},
Suhairi Rizuan Che Ahmad³, Fairul Azhar Abdul Shukor^{1,2}, Md. Nazri Othman^{1,2}

¹Fakulti Teknologi dan Kejuruteraan Elektrik, Universiti Teknikal Malaysia Melaka, Melaka, Malaysia

²Electric Vehicle, Power Electronics, Electric Machine Design and Drives Research Group, Universiti Teknikal Malaysia Melaka, Melaka, Malaysia

³Universiti Kuala Lumpur-British Malaysian Institute (UNIKL-BMI), Selangor, Malaysia

Article Info

Article history:

Received Dec 19, 2024

Revised Jul 2, 2025

Accepted Sep 2, 2025

Keywords:

Food processing

Linear actuator

Linear DC motor

Presser

Slot-less

ABSTRACT

This paper introduces a portable and user-friendly innovation in food processing by replacing traditional molding methods with a linear DC motor (LDM). Traditional methods, which involve manual pressing, are energy-intensive and time-consuming, reducing productivity. The proposed LDM offers a simple, cost-effective, and robust solution capable of producing constant thrust, unlike conventional LDMs that require complex and expensive control methods and are limited to short displacements. The research focuses on modelling and analyzing an LDM with constant thrust characteristics for food processing applications. The primary objective is to model the thrust using the permeance analysis method (PAM), ensuring constant thrust capability. Verification was conducted using the finite element method (FEM) and measurement results, showing a percentage difference of 1.7% and 6.5%, respectively, between PAM and the other methods. The study provides valuable guidance for designing LDMs with constant thrust capabilities, enhancing the efficiency and practicality of food processing devices.

This is an open access article under the [CC BY-SA](#) license.



Corresponding Author:

Raja Nor Firdaus Kashfi Raja Othman

Fakulti Teknologi dan Kejuruteraan Elektrik, Universiti Teknikal Malaysia Melaka

Hang Tuah Jaya Street, 76100 Durian Tunggal, Melaka, Malaysia

Email: norfirdaus@utem.edu.my

1. INTRODUCTION

Linear actuator (LA) has been widely used in the industry for various applications such as aerospace, railway transportation, electric vehicle, agriculture, pumping system, and air compressor [1]-[7]. Recently, demand of portable devices in food and beverage processing has encouraged more LA to be used for such applications [8]-[12]. Traditional devices of portable food pressers that are commonly utilized by the community are shown in Figure 1 [13]. The compression module is divided into two main parts, known as the chamber and plunger. When the dough is being applied inside the chamber, the plunger will compress the dough according to the applied external force by the human, thus producing the resultant dough. Nowadays, a typical linear actuator (TLA) has been used to replace the traditional devices of portable food processing applications [14]-[17]. TLA uses a rotational motor connected to gears and ball screws. When the shaft of the rotational motor rotates, the gears and ball screws rotate as well, thus the rod or plunger starts to move in a translation motion. The assembly of TLA with the external chamber shows that the system requires more space, even though it protects the food material from the gear, ball screw, and grease inside the actuator itself. Thus, TLA is not practical for a simple and portable application.

For such reasons, the authors proposed a new direct contact linear DC motor (LDM) to replace TLA that allows the dough to be compressed inside the LDM itself without compromising the cleanliness, as shown in Figure 2. The absence of a gear and ball screw allows a direct contact motion. The mover and coil casings are made from aluminum and plastic, respectively. This will ensure the cleanliness of the dough even if it is in direct contact with the mover itself.

For this application, the desired LDM that uses a DC supply as its main source should produce a constant thrust characteristic along the mover displacement. Figure 3 shows the comparison of thrust characteristics between a typical LDM and the proposed LDM. The typical LDM has a single peak of thrust characteristics over displacement compared with the proposed LDM, which produces constant displacement. In typical LDM, the compression time is not periodically stable when it operates from the starting position to the end. This will affect the quality of the dough. To overcome the problem, a new LDM needs to be modelled with constant thrust characteristics over displacement.

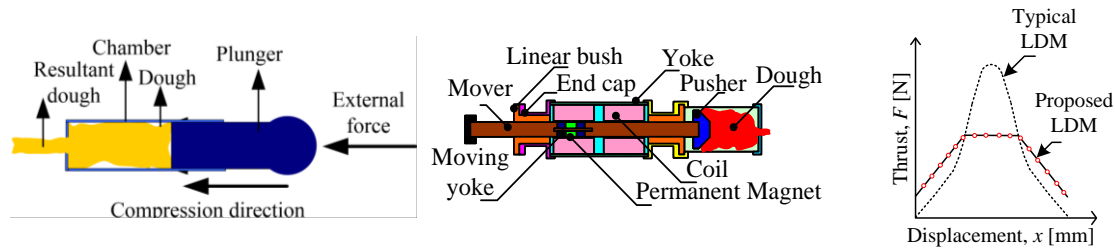


Figure 1. Traditional food presser devices

Figure 2. Proposed new direct contact linear actuator

Figure 3. Thrust characteristics of typical and proposed LDM

Many studies have extended the research on thrust characteristics of linear motors. For instance, Cheema *et al.* [18] proposed a direct thrust control (DTC) of a linear permanent magnet motor. They aimed to reduce the ripple in flux for achieving smoother thrust characteristics. Furthermore, Zhu *et al.* [19] studied several tabular linear permanent magnet machines that used a partitioned stator. Their research was to present the effect of a partitioned stator on the thrust characteristics of the motor. In addition, Jiao *et al.* [20] published a paper on a linear permanent magnet vernier machine.

Their research improved the force density of the linear motor with the implementation of a Hall-Bach array of permanent magnets. For LDM, Zhao *et al.* [21] discussed the dynamic analysis of a moving magnet actuator. They had presented a simulation and experimental approach for predicting the force of the actuator with and without a spring condition. Meanwhile, Hassan *et al.* [22] designed a tabular linear oscillatory motor with the Hall-Bach magnet array. They compared the thrust characteristics with various types of permanent magnet arrays.

There are lots of studies not limited to those mentioned above regarding linear motor and linear DC motor. However, most of them focused on developing a linear actuator with the high-power density using a single or more current phase for longer displacement [22]. In the case of LDM with using DC, most of the literature focused on developing precision and short stroke displacement. None of them focused on improving the stable thrust characteristics and longer stroke of displacement.

This paper focuses on the modeling and analysis of a LDM with constant thrust for food processing applications. The research addresses the gap in conventional LDMs, which typically use a single phase to achieve constant thrust characteristics. Traditionally, multiphase systems have been employed to maintain constant thrust in LDMs using a DC supply. The LDM discussed here is an innovative power molding device designed for the production of traditional cookies, with a particular emphasis on portability—a feature lacking in previous designs. Conventional LDMs exhibit a single peak thrust characteristic relative to displacement, which is unsuitable for portable devices used in food processing. Therefore, the primary objective of this project is to model the thrust of the LDM using the permeance analysis method (PAM) to achieve constant thrust and extended displacement characteristics. A prototype LDM was developed as part of this research, and its performance was verified using the finite element method (FEM) and measurement results. Ultimately, this paper offers guidelines for designing an LDM with constant thrust characteristics, applicable to various uses: i) Section 2 describes the research method of this paper. It describes the basic structure and the specification of the LDM. Then, 2.2 describes the modeling and magnetic circuit of LDM. The modeling of LDM is using PAM based on the flux path in the LDM and based on the flux, the magnetic circuit will be constructed; ii) Section 3 is discussed about the result and discussion. It includes the analysis, prototype and the validation; and iii) Last section will conclude this research.

2. RESEARCH METHOD

2.1. Basic structure and specification

The basic structure of a typical LDM is shown in Figure 4. It has a symmetrical structure for each pole with a stator and a moving part. The stator part consists of a back yoke and coils while the moving part consists of permanent magnets, moving yokes, and a shaft. The criteria to design LDM to operate, the displacement coefficient, α must be designed to be half of the displacement length. This is to ensure that thrust still can be produced until the end of the LDM shaft displacement.

Normally, the permanent magnet is arranged back-to-back so that the flux will flow above towards the center of the coil. The coil is connected in series or parallel connection, but each coil must be in a different pole configuration. This means that each coil must be supplied with a different current direction from the other. When the flux is generated by the coil current, the flux at the right side of the mover is strengthened, and the flux at the left side of the mover is weakened. Thus, a thrust towards the right direction is generated.

Basically, the thrust in the same direction is promoted by Fleming's left-hand rule because the coil current flows perpendicularly to the flux of the permanent magnet. Therefore, when alternating the current flows in the coil, the mover moves to the right and left directions. This basic principle of LDM is illustrated in Figure 5. The right motion of LDM is shown in Figure 5(a). It means that the flux flows from the south pole to the north pole. Meanwhile, Figure 5(b) shows the moving direction is from left motion which is flux flow from the north pole to the south pole.

Figure 6 shows the basic structure of LDM for this research. The basic structure of LDM consists of a stator, moving yokes, coils, a permanent magnet, and a shaft. SS400 steel was used for the stator and moving yokes. Meanwhile, NdFeB35 and SUS304 were used for the permanent magnet and mover, respectively. There are several selected parameters fixed and varied in order to achieve the target performance of the designed LDM. The LDM was intended for portable application. Table 1 shows the fixed parameters obtained from the preliminary experiment, whereas Table 2 shows the variable parameters calculated based on the desired specification.

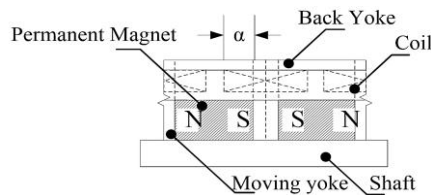


Figure 4. The cross-sectional view of typical LDM

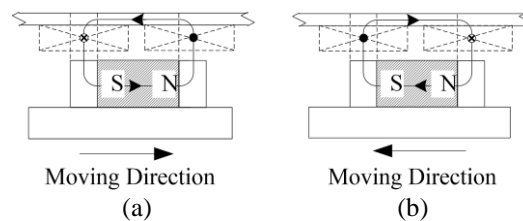


Figure 5. Basic principle of LDM: (a) right motion and (b) left motion

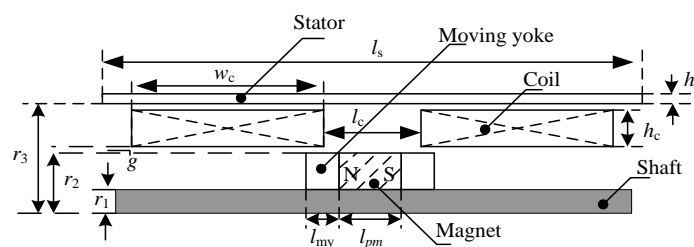


Figure 6. Basic structure of LDM in this research

Table 1. The fixed parameter of LDM Table 2. The variable parameter of LDM

Element	Values [MM]
l_s	183
h_s	4
l_{pm}	20
l_{my}	8
g	0.5
r_1	5

Element	Values [MM]
l_s	55, 60, 65
w_c	10.5, 11.5, 12.5
h_c	13, 14, 15
r_2	26, 27, 28
r_3	5, 10, 15, 20, 25, 30
l_c	55, 60, 65

The target performance of the proposed LDM for food processing application is shown in Figure 7. The displacement at constant thrust is known as effective displacement x_{op} . The target x_{op} and thrust are ≥ 30 mm and 80 N respectively. The target performance was obtained from the preliminary experiment conducted with the industry. The preliminary experiment involved a traditional molding device that had been used by the community to produce traditional cookies such as tart and samperit.

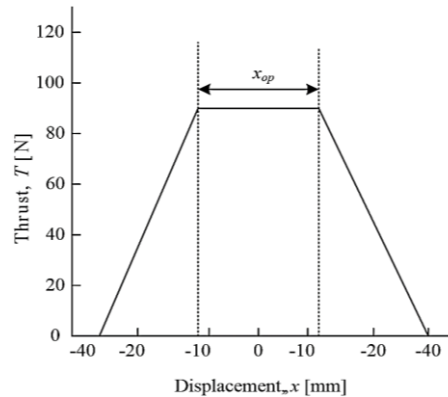


Figure 7. Target performance of designs LDM

2.2. Modeling and magnetic circuit

Permeance analysis method (PAM) is one of the methods that can be used to model the thrust characteristic related to the electromagnetics and physical size of LDM. The modeling developed in this research can be used to calculate the thrust of the other linear machine that has a similar structure to LDM. Figure 8(a) shows the flux lines of LDM at 0 mm position of the mover which simulated by using FEM of the Ansys Maxwell software. Basically, the thrust is not maximum at the central point but this point is selected to be discussing in this paper to analyze the effect of magnetic flux when permanent magnet is placed between coils. From the analysis, the constant thrust produced when the flux is not symmetry at both right and left side. Besides that, the thrust starts to decrease when both flux of left and right start to symmetry each other. There are two flux lines considered in this PAM which are at the left and right sides. Nevertheless, the permeances models were built depending on the estimated flux path at the air gap (including coil) by assuming that the permeability of the yoke was regarded as infinity [23].

All flux lines must be mutually perpendicular at each point of intersection [24]. Each figure was bounded by two adjacent flux lines while two adjacent equipotential lines must be in curvilinear square. The width ratio of the average width to the average height of each square should be equal to unity. Figure 8(b) shows the simplified flux lines of LDM in this research. The resulting flux lines were observed at 0 mm position of the mover. It was recognized that it has two paths of flux lines which are the left and right side of LDM.

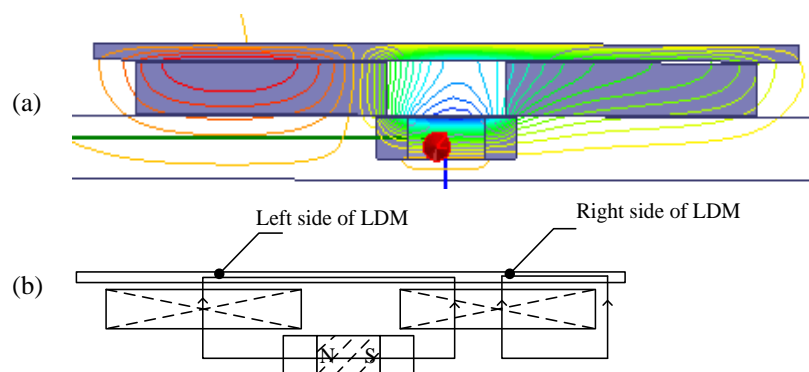


Figure 8. The path of flux of LDM in this research: (a) the flux lines of LDM simulated by FEM and (b) simplified flux lines of LDM for PAM

Figure 9 is the developed permeance models for LDM in this research. The permeance equation is different for every displacement of the mover. Figure 9(a) shows the permeance model of LDM for this

research. The permeance model was only considered at zero displacement of a mover because at this point the designed motor has constant thrust characteristics. While Figure 9(b) is obtained from the region of the flux leakage above the permanent magnet. Figure 10 is the magnetic equivalent circuit at the left and right sides of flux lines of the permeances model. At the left side of LDM, there were ten permeance models but at the right side, there were only three permeance models.

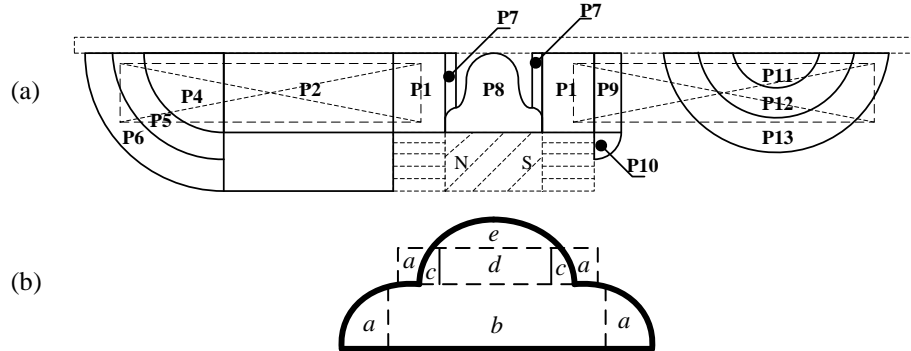


Figure 9. The permeance model of LDM in this research: (a) permeance model and (b) details of permeances 8

Basically, the permeance value can be calculated based on the developed permeance equation in the permeance model. The equation of the permeance model is based on the basic formula of the permeance shape. The (1) provides the basic formula in permeance:

$$P = \frac{\mu_0 a}{l} \text{ [H]} \quad (1)$$

where P is the permeance value in (H), μ_0 is the air permeability in (H/m), a is the air gap area in (m^2), and l is the gap length in (m).

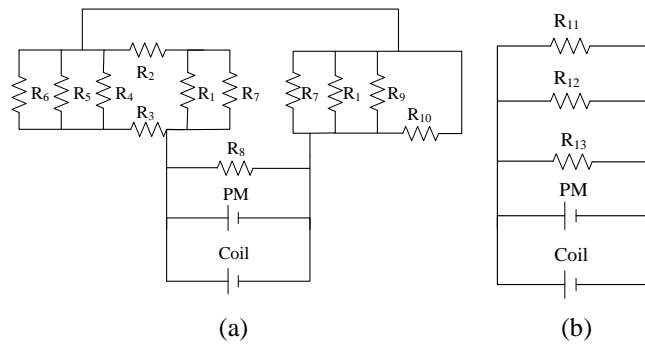


Figure 10. The magnetic equivalent circuit of LDM: (a) left side and (b) right side

By referring to the basic formula and based on the shape of the permeance model, it can be denoted as (2)-(21).

$$P_1 = \frac{\mu_0 l m y}{\pi} \ln(1 + (r_3 - r_2)) \text{ [H]} \quad (2)$$

$$P_2 = \frac{\mu_0 (r_3 - r_2)}{\pi} \ln\left(1 + \frac{w_c}{2}\right) \text{ [H]} \quad (3)$$

$$P_3 = \frac{\mu_0 (r_2 - r_1)}{\pi} \ln\left(1 + \frac{w_c}{2}\right) \text{ [H]} \quad (4)$$

$$P_4 = 0.52 \mu_0 \left(r_2 + \frac{r_3 - r_2}{2}\right) \text{ [H]} \quad (5)$$

$$P_5 = \frac{\mu_o 2 \left[2\pi \left[r_1 + \left(\frac{r_2 - r_1}{2} \right) + \frac{r_3 - \left(r_1 + \frac{r_2 - r_1}{2} \right)}{2} \right] \right]}{\pi} \times \ln \left(1 + \frac{r_2 - r_1}{r_3 - r_2} \right) \quad [\text{H}] \quad (6)$$

$$P_6 = \frac{\mu_o (2) \left[2\pi \left(r_1 + \frac{r_3 - r_1}{2} \right) \right]}{\pi} \ln \left(1 + \frac{\frac{r_2 - r_1}{2}}{r_3 - \left(r_1 + \frac{r_2 - r_1}{2} \right)} \right) \quad [\text{H}] \quad (7)$$

$$P_7 = \left[(0.52) \mu_o \left(2\pi \left(r_2 + \frac{g}{2} \right) \right) \right] - \left[\frac{\mu_o g}{\pi} \ln \left(1 + \frac{2(r_3 - r_2)}{2r_2} \right) \right] 2 \quad [\text{H}] \quad (8)$$

$$a = 0.52 \mu_o \left[2\pi \left(r_2 + \frac{g}{2} \right) \right] \quad [\text{H}] \quad (9)$$

$$b = \left[\frac{\mu_o (l_{pm} - 2g)}{\pi} \ln \left(1 + \frac{2g}{2r_2} \right) \right] 2 \quad [\text{H}] \quad (10)$$

$$c = \left[0.52 \mu_o \left(2\pi \left(r_2 + \frac{g}{2} \right) \right) \right] - \left[\frac{\mu_o g}{\pi} \ln \left(1 + \frac{2g}{2(r_2 + g)} \right) \right] 2 \quad [\text{H}] \quad (11)$$

$$d = \left[\frac{\mu_o \frac{6h_c}{10}}{\pi} \ln \left(1 + \frac{2g}{2(r_2 + g)} \right) \right] 2 \quad [\text{H}] \quad (12)$$

$$e = 0.52 \mu_o \left[2\pi \left(r_3 - \frac{3h_c}{10} \right) \right] \quad [\text{H}] \quad (13)$$

$$P_8 = \left[\frac{1}{\frac{1}{a} + \frac{1}{c}} \right] + \left[\frac{1}{\frac{1}{c} + \frac{1}{d}} \right] + e \quad [\text{H}] \quad (14)$$

$$P_9 = \frac{\mu_o \frac{w_c}{10}}{\pi} \ln(1 + (r_3 - r_2)) \quad [\text{H}] \quad (15)$$

$$P_{10} = 0.52(\mu_o) \left(r_1 + \frac{r_2 - r_1}{4} \right) \quad [\text{H}] \quad (16)$$

$$P_{11} = 1.63 \mu_o \left(h_s + \frac{w_c}{4} \right) \quad [\text{H}] \quad (17)$$

$$P_{12} = \frac{\mu_o (2\pi r_3)}{\pi} \ln \left(1 + \frac{2 \left(\frac{w_c}{9} \right)}{2 \left(\frac{w_c}{9} \right)} \right) \quad [\text{H}] \quad (18)$$

$$P_{13} = \frac{\mu_o (2\pi r_3)}{\pi} \ln \left(1 + \frac{2 \left(\frac{w_c}{9} \right)}{4 \frac{w_c}{9}} \right) \quad [\text{H}] \quad (19)$$

The total permeance for magnetic equivalent circuit for left and right side are shown as:

$$\frac{1}{P_{T(left)}} = \frac{(P_2 + P_3 + P_4 + P_5 + P_6)}{P_2 P_3 (P_4 + P_5 + P_6) + P_1 (P_2 + P_3 + P_4 + P_5 + P_6) + P_7 (P_2 + P_3 + P_4 + P_5 + P_6)} + \frac{1}{P_8} + \frac{1}{(P_1 + P_7 + P_9 + P_{10})} \quad [\text{H}] \quad (20)$$

$$P_{T(right)} = P_{11} + P_{12} + P_{13} \quad [\text{H}] \quad (21)$$

Considering that the permanent magnet has demagnetization curve as shown in Figure 11 [25]. It has a remanent magnetic flux density of B_r and a coercive force of H_c . The total permeance, for each magnetic equivalent circuit used to determine a slope of a linear line called permeance line. An intersection point between these two lines is called the operating point of permanent magnet or K point. At this point, it will give a value of operating magnetic flux density of permanent magnet, B_k .

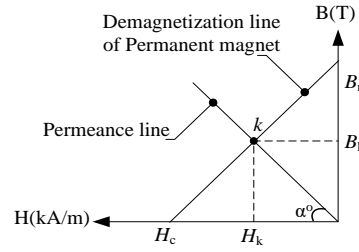


Figure 11. The demagnetization curves

The slope of a permeance line depends on the α angle. The α is given by (22).

$$\tan \alpha = \frac{B_r H_c l_{pm}}{2 B_r A_M} \quad (22)$$

The equation of permeance line can be denoted as (23).

$$B_k = (\tan \alpha)(H_k) \quad (23)$$

The demagnetization curve of permanent magnet can be represented by the linear as in (24).

$$B = \frac{B_r}{H_c} H + B_r \quad (24)$$

The value of B_k and H_k can be determined by solving in (23) and (24), respectively. The flux of the permanent magnet at the airgap can be represented as (25).

$$\phi_m = B_k A_m \quad [\text{Wb}] \quad (25)$$

Given that n is the magnetic circuit on the left or right side. Since the thrust of LDM was produced at the center of coil, and assuming all flux flow towards the coil thus:

$$\phi_c = \phi_m \quad [\text{Wb}] \quad (26)$$

$$B_{k(n)} = \frac{\phi_c}{A_c} \quad [\text{T}] \quad (27)$$

$$F_{(n)} = N_c I_c B_{k(n)} l_c \quad [\text{N}] \quad (28)$$

$$F_T = F_{(left)} + F_{(right)} [\text{N}] \quad (29)$$

whereas a , b , c , d , and e are the permeance values of region 8 in [H], B_r is the magnetic remanence in [T], B_k is the operating magnetic flux density of permanent magnet in [T], $B_{k(n)}$ is the magnetic flux density of coil in [T], n is the coil at the left or right side, H_c is the coercive force in [A/m], H_k is the operating coercive force of permanent magnet in [A/m], α is the angle of demagnetization curve in $^\circ$, A_m is the area of magnet in $[\text{m}^2]$, A_c is the area of coil in $[\text{m}^2]$, l_c is the length of coil in $[\text{m}^2]$, ϕ_m is the flux of permanent magnet in [Wb], ϕ_c is the flux of coil in [Wb], $F_{(n)}$ is the force produced in [N], F_T is the total force produced in [N], $F_{(left)}$ is the force produced at the left side of magnetic circuit in [N], $F_{(right)}$ is the force produced at the right side of the magnetic circuit in [N], N_c is the number of turn of coil and I_c is the supplied current at the coil in [A].

3. RESULTS AND DISCUSSION

3.1. Analysis

Several analyses were conducted by changing the dimension of the varied parameters. From the analysis, constant thrust can be achieved along the effective displacement x_{op} when l_c is varied. The result of the analysis is as in (30).

$$x_{op} = l_c \quad [N] \quad (30)$$

This is because as the l_c is getting wider, there are no significant changes of flux, which means that there are no changes of $B_{k(n)}$ which contribute to the production of thrust. This allows constant thrust along the effective displacement x_{op} . The increasing values of w_c , h_c , r_2 , r_3 , will increase the value of thrust as these affect the dimensions of coil and permanent magnet sizes. These values do not affect the shape of the thrust characteristic waveform. The prototype of LDM was fabricated for experimental validation, as shown in Figure 12.

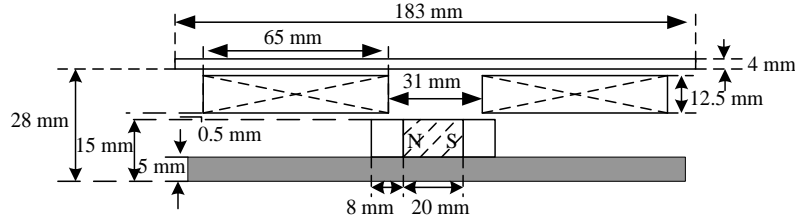


Figure 12. Selected model of LDM for fabrication

3.2. Prototype

Figure 13(a) shows the prototype of LDM in this research. The advantage of using LDM is a higher average thrust. Figure 13(b) is the experimental setup of the prototype LDM. The mover is attached with a load cell to measure the resulting amount of force when the mover moves. The resistance value of the coil is 17Ω and the number of turns of each coil is 1206.

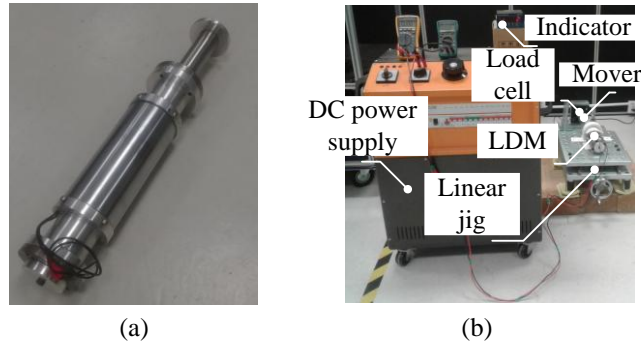


Figure 13. Prototype of LDM for food processing application: (a) prototype and (b) experimental setup

3.3. Validation

Figure 14 shows the frequency characteristics for LDM coils at a mover position of 50 mm. Basically, there are two coils which connected in series to equalize the current flowing inside the design LDM. The frequency characteristics were measured by using LCR meter. Fundamentally, the LCR meter shows the value of inductance, L and resistance, R only for range of frequency between 12 Hz until 100 kHz. While, for the others parameters such as phase difference, θ and impedance, Z was calculated as in (31) and (32).

$$\theta = \cos^{-1} \left(\frac{R}{Z} \right) \quad (31)$$

$$Z = \sqrt{R^2 + (j\omega L)^2} \quad (32)$$

Based on the result obtain, the frequency of power supply in LDM is suggested to be below than 100 Hz because the value of resistance is stable and low at this range of frequency. It is also will help to minimize the usage of power rating and reduce the consumption of electricity.

Figure 15 shows comparison of performance using FEM, PAM, and the measurement result in LDM for validation purpose. Fundamentally, the result of FEM is the most accurate and must be higher comparing with others methods. While the PAM result must be lower than FEM but higher than experimental. It is

because of PAM will have an error about 6.5 % lower than FEM. The experimental result is the lowest because the existence of the friction force due to high normal thrust produced by LDM. While, the constant thrust has a certain ripple in FEM is because of the setting at the analysis setup during analysis process. For smooth waveform, the time step should be reducing as small as possible. The PAM methods can catch the ripple if more permeance model were developing for every position of the mover. Thus, the PAM methods can produce similar characteristics as FEM which is basically more accurate. Moreover, to reduce the ripple in experimental, the thrust value should be measured in small displacement as possible.

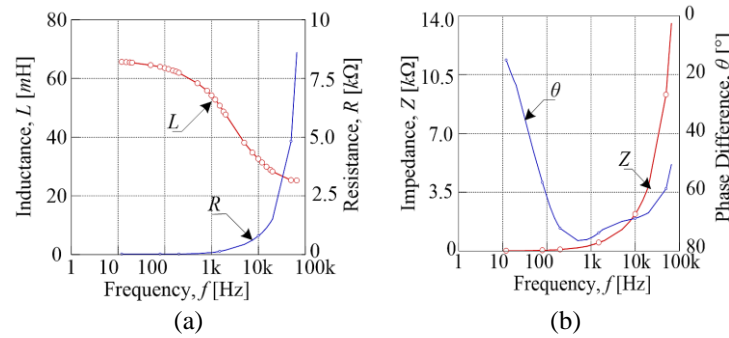


Figure 14. Frequency characteristics for prototype of LDM: (a) effect of L & R , and (b) effect of θ & Z

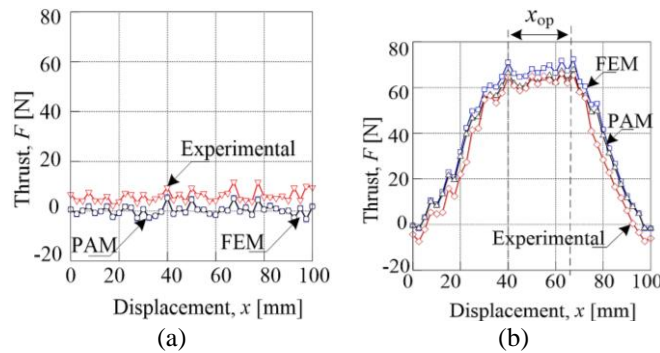


Figure 15. Comparison of performance in LDM for validation: (a) cogging thrust, and (b) thrust at $i = 6$ A

By referring to the graph of cogging thrust, the experimental result higher than the PAM and FEM because 20 kgf capacity of load cell had been used in this research. In fact for the accuracy, low capacity of load cell should be implied in low current, instead it is not appropriate to be measured for higher current. The load cell of 20 kgf is used in this research to synchronize the entire measured current, i. Based on Figure 15(a), the percentage difference between PAM with FEM and the measurement result is 6.5% and 1.7% respectively. It can be seen that the constant thrust among the displacement, x_{op} has only a small significant difference values among these three methods. All three methods were in good agreement of each other. Table 3 summarizes the validation of LDM at position 50 mm. Figure 15(b) shows the thrust produced when current is injected 6A. The percentage difference between PAM and FEM is about 5.6%. Meanwhile, the percentage difference between PAM and measurement is 1.5%. The percentage difference between them is less than 10% which marked this method is significant method to do the comparison.

Table 3. The LDM performance

Method	Constant thrust [N]	Displacement, x_{op} [mm]
FEM	68	30
PAM	63.67	30
Measured	59	27.5

4. CONCLUSION

For modeling the constant thrust the LDM, the PAM is used and will be simulated using FEM known as Ansys Maxwell. The result from PAM and FEM is validated with the measurement result. The

LDM was designed for food processing application. It shows that the percentage difference between PAM with FEM and measurement result was 6.5% and 1.7% respectively. The constant thrust can be achieved along the effective displacement x_{op} when l_c is varied. Academically, this paper provides guidance on designing an LDM for a constant thrust capability using PAM. Therefore, it is believed that this LDM is suitable for food processing devices which could contribute to the wealth and economy of the food industry.

ACKNOWLEDGEMENTS

Author would like to thank Ministry of Higher Education and Universiti Teknikal Malaysia Melaka (UTeM) for financial support for this research.

FUNDING INFORMATION

The authors would like to thank various parties such as Ministry of Higher Education and Universiti Teknikal Malaysia Melaka (UTeM) for Fundamental Research Grant Scheme (FRGS/1/2015/TK04/FKE/02/F00260) and UTeM Publication Initiative 2025 Scheme for journal publication fees.

AUTHOR CONTRIBUTIONS STATEMENT

This journal uses the Contributor Roles Taxonomy (CRediT) to recognize individual author contributions, reduce authorship disputes, and facilitate collaboration.

Name of Author	C	M	So	Va	Fo	I	R	D	O	E	Vi	Su	P	Fu
Raja Nor Firdaus	✓	✓		✓	✓	✓	✓	✓	✓	✓	✓	✓	✓	
Kashfi Raja Othman														
Siti Zulaika Mat Isa	✓	✓	✓	✓	✓	✓		✓	✓	✓	✓	✓		
Nor Aishah Md. Zuki	✓		✓	✓	✓					✓	✓			
Suhairi Rizuan Che		✓		✓		✓				✓			✓	
Ahmad														
Fairul Azhar Abdul					✓		✓			✓		✓	✓	
Shukor														
Md. Nazri Othman		✓			✓		✓			✓		✓	✓	

C : Conceptualization

M : Methodology

So : Software

Va : Validation

Fo : Formal analysis

I : Investigation

R : Resources

D : Data Curation

O : Writing - Original Draft

E : Writing - Review & Editing

Vi : Visualization

Su : Supervision

P : Project administration

Fu : Funding acquisition

CONFLICT OF INTEREST STATEMENT

The authors declare no conflict of interest.

DATA AVAILABILITY

Data availability does not apply to this paper as new data were created or analyzed in this study.





REFERENCES

- [1] A. L. Shurajji, Z. Q. Zhu, and Q. F. Lu, "A novel partitioned stator flux reversal permanent magnet linear machine," *IEEE Transactions on Magnetics*, vol. 52, no. 1, pp. 1–6, Jan. 2016, doi: 10.1109/TMAG.2015.2478492.
- [2] C.-T. Liu, Y.-W. Chiu, and C.-C. Hwang, "Designs and feasibility assessments of an integrated linear electromagnetic actuator for cold roll mill applications," *IEEE Transactions on Industry Applications*, vol. 52, no. 3, pp. 2693–2699, May 2016, doi: 10.1109/TIA.2016.2526959.
- [3] K. Okada and K. Akatsu, "Design of axial type slot-less PMSM and systems for electric wheelbarrow," in *2015 18th International Conference on Electrical Machines and Systems (ICEMS)*, IEEE, Oct. 2015, pp. 830–835. doi: 10.1109/ICEMS.2015.7385149.
- [4] H. Karimi, S. Vaez-Zadeh, and F. Rajaei Salmasi, "Combined vector and direct thrust control of linear induction motors with end effect compensation," *IEEE Transactions on Energy Conversion*, vol. 31, no. 1, pp. 196–205, Mar. 2016, doi: 10.1109/TEC.2015.2479251.
- [5] M. Norhisam, R. N. Firdaus, F. Azhar, N. Mariun, I. Aris, and R. J. Abdul, "The analysis on effect of thrust constant, spring constant, electrical time constant, mechanical time constant to oscillation displacement of slot-less linear oscillatory actuator," in *2008 IEEE 2nd International Power and Energy Conference*, IEEE, Dec. 2008, pp. 1076–1081. doi: 10.1109/PECON.2008.4762635.




- [6] S. Zhang, L. Norum, and R. Nilssen, "Analysis of tubular linear permanent magnet motor for drilling application," *2009 International Conference on Electric Power and Energy Conversion Systems, EPECS 2009*, 2009.
- [7] S. M. Jang, D. J. You, S. H. Lee, H. W. Cho, and W. B. Jang, "Design and analysis of three types for permanent magnet linear synchronous machine," *ICEMS 2003 - Proceedings of the 6th International Conference on Electrical Machines and Systems*, vol. 1, pp. 31–33, 2003.
- [8] Q. L. Wang, X. Z. Huang, Z. Bo, Q. Tan, and J. Li, "The analysis and compensation control of the detent force for slot-less tubular permanent magnet linear synchronous motor," in *2015 IEEE International Conference on Applied Superconductivity and Electromagnetic Devices (ASEMD)*, IEEE, Nov. 2015, pp. 145–146. doi: 10.1109/ASEMD.2015.7453507.
- [9] Q. Wang, B. Zhou, X. Huang, and Q. Tan, "Suppression of leakage flux and thrust ripple for slot-less tubular permanent magnet linear synchronous motor," in *2014 IEEE Conference and Expo Transportation Electrification Asia-Pacific (ITEC Asia-Pacific)*, IEEE, Aug. 2014, pp. 1–4. doi: 10.1109/ITEC-AP.2014.6940827.
- [10] K. J. W. Pluk, J. W. Jansen, and E. A. Lomonova, "Force measurements on a shielded coreless linear permanent magnet motor," *IEEE Transactions on Magnetics*, vol. 50, no. 11, pp. 1–4, Nov. 2014, doi: 10.1109/TMAG.2014.2327655.
- [11] H. Wakiwaka, T. Ninomiya, J. Oda, T. Morimura, and H. Yamada, "Evaluation of the thrust constant of a linear DC motor for a pen recorder," *IEEE Translation Journal on Magnetics in Japan*, vol. 9, no. 6, pp. 104–109, Nov. 1994, doi: 10.1109/TJMJ.1994.4565965.
- [12] M. Norhisam, K. Alias, R. N. Firdaus, S. Mahmud, N. Mariun, and J. A. Razak, "Comparison on thrust characteristic of linear oscillatory actuators," in *2006 IEEE International Power and Energy Conference*, IEEE, Nov. 2006, pp. 470–475. doi: 10.1109/PECON.2006.346697.
- [13] R. N. Firdaus *et al.*, "Design a slot-less linear actuator for food processing application," *Journal of Telecommunication, Electronic and Computer Engineering*, vol. 8, no. 7, pp. 87–91, 2016.
- [14] A. Ismael and F. J. Anayi, "Modelling of a prototype brushless permanent magnet DC linear stepping motor employing a flat-armature winding configuration," in *2016 Third International Conference on Electrical, Electronics, Computer Engineering and their Applications (EECEA)*, IEEE, Apr. 2016, pp. 88–92. doi: 10.1109/EECEA.2016.7470771.
- [15] Q. Lu, Y. Yao, Y. Ye, and J. Dong, "Research on rope less elevator driven by PMLSM," in *2016 Eleventh International Conference on Ecological Vehicles and Renewable Energies (EVER)*, IEEE, Apr. 2016, pp. 1–6. doi: 10.1109/EVER.2016.7476386.
- [16] B. Kou, J. Luo, X. Yang, and L. Zhang, "Modeling and analysis of a novel transverse-flux flux-reversal linear motor for long-stroke application," *IEEE Transactions on Industrial Electronics*, vol. 63, no. 10, pp. 6238–6248, Oct. 2016, doi: 10.1109/TIE.2016.2581142.
- [17] T. J. Teo, H. Zhu, S.-L. Chen, G. Yang, and C. K. Pang, "Principle and modeling of a novel moving coil linear-rotary electromagnetic actuator," *IEEE Transactions on Industrial Electronics*, vol. 63, no. 11, pp. 6930–6940, Nov. 2016, doi: 10.1109/TIE.2016.2585540.
- [18] M. A. M. Cheema, J. E. Fletcher, D. Xiao, and M. F. Rahman, "A direct thrust control scheme for linear permanent magnet synchronous motor based on online duty ratio control," *IEEE Transactions on Power Electronics*, vol. 31, no. 6, pp. 4416–4428, Jun. 2016, doi: 10.1109/TPEL.2015.2475400.
- [19] Z. Q. Zhu, A. L. Shurajji, and Q. F. Lu, "Comparative study of novel tubular partitioned stator permanent magnet machines," *IEEE Transactions on Magnetics*, vol. 52, no. 1, pp. 1–7, Jan. 2016, doi: 10.1109/TMAG.2015.2476558.
- [20] Z. Jiao, T. Wang, and L. Yan, "Design of a tubular linear oscillating motor with a novel compound halbach magnet array," *IEEE/ASME Transactions on Mechatronics*, vol. 22, no. 1, pp. 498–508, Feb. 2017, doi: 10.1109/TMECH.2016.2611604.
- [21] W. Zhao, J. Zheng, J. Wang, G. Liu, J. Zhao, and Z. Fang, "Design and analysis of a linear permanent- magnet vernier machine with improved force density," *IEEE Transactions on Industrial Electronics*, vol. 63, no. 4, pp. 2072–2082, Apr. 2016, doi: 10.1109/TIE.2015.2499165.
- [22] A. Hassan, A. Bijanzad, and I. Lazoglu, "Dynamic analysis of a novel moving magnet linear actuator," *IEEE Transactions on Industrial Electronics*, vol. 64, no. 5, pp. 3758–3766, May 2017, doi: 10.1109/TIE.2016.2645506.
- [23] D. Wang, C. Shao, and X. Wang, "Design and performance evaluation of a tubular linear switched reluctance generator with low cost and high thrust density," *IEEE Transactions on Applied Superconductivity*, vol. 26, no. 7, pp. 1–5, Oct. 2016, doi: 10.1109/TASC.2016.2599202.
- [24] T. Mizuno, M. Kawai, F. Tsuchiya, M. Kosugi, and H. Yamada, "An examination for increasing the motor constant of a cylindrical moving magnet-type linear actuator," *IEEE Transactions on Magnetics*, vol. 41, no. 10, pp. 3976–3978, Oct. 2005, doi: 10.1109/TMAG.2005.855160.
- [25] T. Mizuno *et al.*, "Considerations on electrical and mechanical time constants of a moving-magnet-type linear dc motor," *Sensors and Actuators, A: Physical*, vol. 81, no. 1, pp. 301–304, 2000, doi: 10.1016/S0924-4247(99)00180-6.

BIOGRAPHIES OF AUTHORS






Raja Nor Firdaus Kashfi Raja Othman     received B.Eng., M.Sc. and Ph.D. in Electrical Engineering from Universiti Putra Malaysia in 2006, 2009 and 2013, respectively. He is currently associate professor in Department of Electrical Power Engineering, Faculty of Electrical Technology and Engineering, Universiti Teknikal Malaysia Melaka. His research interest is applied magnetism, electrical machines, magnetic sensor and drives. He can be contacted at email: norfirdaus@utem.edu.my.






Siti Zulaika Mat Isa    was born on 13 November 1992 at Butterworth, Pulau Pinang. In 2018, she received her Master of Science in Electrical Engineering from Universiti Teknikal Malaysia Melaka (UTeM). Currently, she is working as Electrical Engineer at Infineon Technologies (Kulim) Sdn Bhd. Her work environment is focused on electrical distribution, 132 kV & 33 kV upstream, 11 kV downstream, control system, electrical final distribution, genset and DDUPS system, and energy management topics as Registered Electrical Energy Manager (REEM-PTE-0208-2024). She can be contacted at email: sitizulaika.matisa@infineon.com.






Nor Aishah Md. Zuki    was born on 9 November 1992 in Kuantan, Pahang, Malaysia. In 2018, she received her Master of Science in Electrical Engineering from Universiti Teknikal Malaysia Melaka (UTeM). Currently, she is pursuing her study in Ph.D. from the same university. Her research study is on machine design. She can be contacted at email: p011820006@student.utem.edu.my.






Suhairi Rizuan Che Ahmad    was born on 13 June 1984 at Kota Bharu, Kelantan. He received the B.Eng. in Industrial Electronics from Universiti Malaysia Perlis, Malaysia in 2009 and M.Sc. degrees in electrical power engineering from Universiti Putra Malaysia, Malaysia in 2012. In 2019, he received his Ph.D. degree from Universiti Teknikal Malaysia Melaka, Durian Tunggal, Malaysia, in electrical machine design. His research interests are electrical machine design, electric machine simulation, electric drives, energy conversion, and renewable energy. He can be contacted at email: suhairir@unikl.edu.my.



Fairul Azhar Abdul Shukor    is a senior lecturer at the Faculty of Electrical Technology and Engineering, Universiti Teknikal Melaka, Malaysia (UTeM), Melaka. He has been with UTeM since 2005. He received his B.Eng. Degree in Electrical and Electronic Engineering and M.Sc. in Electrical Engineering from Universiti Putra Malaysia in 2002 and 2009, respectively. In 2009, he received his Ph.D. Eng. in machine design from Shinshu University, Japan. His areas of interest include electrical machine and actuator design, numerical analysis, and machine drive. He can be contacted at email: fairul.azhar@utem.edu.my.



Md. Nazri Othman    received his B.Sc. degree in electrical power from Memphis State University, United States, M.Sc. degree in power electronics and drives, and Ph.D. degree in electrical engineering from the University of Nottingham, United Kingdom. Currently, he is serving as a lecturer at UTeM, Malaysia. His research interests are electric machine design and renewable energy. He can be contacted at email: nazri@utem.edu.my.